Original Article
Mol Imaging Radionucl Ther 2021;30:69-78 DOI:10.4274/mirt.galenos.2021.08831

Pharmacokinetic Modeling of ^{18}F-FDOPA PET in the Human Brain for Early Parkinson's Disease

Erken Parkinson Hastalığının İnsan Beyninde ^{18}F-FDOPA PET Yöntemiyle Farmakokinetik Modellemesi

Wirunpatch Buratachwatanasiri[1,2], Maythinee Chantadisai[3], Jaruwan Onwanna[2,4], Yuda Chongpison[5], Yothin Rakvongthai[1,2,3], Kitiwat Khamwan[1,2,3]

[1]*Medical Physics Program, Department of Radiology, Faculty of Medicine, Chulalongkorn University, Bangkok, Thailand*
[2]*Chulalongkorn University Biomedical Imaging Group, Department of Radiology, Faculty of Medicine, Chulalongkorn University, Bangkok, Thailand*
[3]*Division of Nuclear Medicine, Department of Radiology, Faculty of Medicine, Chulalongkorn University and King Chulalongkorn Memorial Hospital, The Thai Red Cross Society, Bangkok, Thailand*
[4]*Biomedical Engineering Program, Faculty of Engineering, Chulalongkorn University, Bangkok, Thailand*
[5]*Center of Excellence in Biostatistics, Research Affairs, Faculty of Medicine, Chulalongkorn University, Bangkok, Thailand*

Abstract

Objectives: Early detection is essential for the treatment approaches of Parkinson's disease (PD). Clinical criteria alone may be insufficient to distinguish early PD from other conditions. This study aimed to investigate the transfer rate constants of 6-^{18}F-fluoro-L-dopa (^{18}F-FDOPA) in positron emission tomography (PET) brain images as a sensitive parameter to detect early PD.

Methods: Retrospective ^{18}F-FDOPA PET data of five patients with early PD were collected. PET data were acquired for 90 min after intravenous injection of 306-379 MBq ^{18}F-FDOPA, and reconstructed into a series of 18 five-minute frames. Reoriented PET images were coregistered and normalized with the PET brain template on the statistical parametric mapping. The ^{18}F-FDOPA activity concentrations were measured in the striatum, caudate, and putamen on both sides: Contralateral (as PD) and ipsilateral (as control) to the main motor symptoms. The pharmacokinetic model was generated using the SAAM II simulation software. The transfer rate constants across the blood-brain barrier (forward, K_1 and reverse, k_2) and decarboxylation rate constants (k_3) were estimated in these regions.

Results: The activity uptakes in the contralateral striatum (0.0323%±0.0091%) and putamen (0.0169%±0.0054%) were significantly lower than the control (0.0353%±0.0086%, 0.0199%±0.0054%, respectively). The K_1 and k_3 were significantly lower in the contralateral striatum and putamen ($p<0.05$). There were no significant differences in any transfer rate constants in the caudate.

Conclusion: The transfer rate constants (K_1 and k_3) of ^{18}F-FDOPA on the contralateral striatum and putamen were significantly lower than the control. These biokinetic data could be potential indicators for quantitative detection of early PD diagnosis.

Keywords: ^{18}F-FDOPA, early Parkinson's disease detection, pharmacokinetic model, statistical parametric mapping, quantitative analysis

Address for Correspondence: Kitiwat Khamwan PhD, Division of Nuclear Medicine, Department of Radiology, Faculty of Medicine, Chulalongkorn University and King Chulalongkorn Memorial Hospital, The Thai Red Cross Society, 1873 Rama IV Road, Pathumwan, Bangkok 10330, Thailand
Phone: +66-61-9325919 **E-mail:** kitiwat.k@chula.ac.th ORCID ID: orcid.org/0000-0001-6247-2829
Received: 14.12.2020 **Accepted:** 01.04.2021

Öz

Amaç: Parkinson hastalığının (PH) tedavi yaklaşımında erken tanı önemlidir. Klinik kriterler tek başına erken PH'yi diğer nedenlerden ayırt etmek için yetersiz olabilir. Bu çalışmada, 6-^{18}F-floro-L-dopa (^{18}F-FDOPA) pozitron emisyon tomografisi (PET) beyin görüntülemede transfer hızı sabitlerinin erken PH saptanmasında duyarlı bir parametre olup olmadığının araştırılması amaçlanmıştır.

Yöntem: Erken PH'li beş hastanın geriye dönük ^{18}F-FDOPA PET verileri toplandı. PET verileri, 306-379 MBq ^{18}F-FDOPA'nın intravenöz enjeksiyonundan sonra 90 dakika süreyle alındı ve 18 adet beşer dakikalık bir dizi halinde rekonstrükte edildi. Reoryante edilen PET görüntüleri istatistiksel parametrik haritalama üzerindeki beyin PET şablonu ile birleştirildi ve normalize edildi. ^{18}F-FDOPA aktivite konsantrasyonları her iki tarafta striatum, kaudat ve putamende ölçüldü: Ana motor semptomlara karşı kontralateral (PH olarak) ve ipsilateral (kontrol olarak). Farmakokinetik model SAAM II simülasyon yazılımı kullanılarak geliştirildi. Bu bölgelerde kan-beyin bariyeri boyunca transfer hızı sabitleri (ileri, K_1 ve geri, k_2) ve dekarboksilasyon hızı sabitleri (k_3) tahmini ölçümleri yapıldı.

Bulgular: Kontralateral striatumda (%0,0323±%0,0091) ve putamende (%0,0169±%0,0054) aktivite alımları kontrolden anlamlı derecede düşüktü (sırasıyla; 0,0353%±0,0086%, 0,0199%±0,0054%). K_1 ve k_3 kontralateral striatum ve putamenlerde anlamlı derecede düşüktü ($p<0,05$). Kaudattaki herhangi bir transfer hızı sabitinde anlamlı bir fark yoktu.

Sonuç: Kontralateral striatum ve putamendeki ^{18}F-FDOPA'nın transfer hızı sabitleri (K_1 ve k_3) kontrolden anlamlı derecede düşüktü. Bu biyokinetik veriler, erken evre PH tanısının kantitatif tespiti için potansiyel göstergeler olabilir.

Anahtar kelimeler: ^{18}F-FDOPA, erken Parkinson hastalığı tespiti, farmakokinetik model, istatistiksel parametrik haritalama, kantitatif analiz

Introduction

Parkinson's disease (PD) is the second most common neurodegenerative disorder. Degeneration of dopamine neurons in the mesencephalic substantia nigra causes the progressive impairment of dopaminergic innervations of the caudate or putamen. When over 50% of the nigrostriatal dopamine neurons have degenerated, PD symptoms are usually distinctly expressed, such as resting tremor, bradykinesia, and rigidity (1,2,3,4). In the early PD stage, clinical criteria alone may be insufficient to distinguish PD from other conditions such as parkinsonism-related disorders or other drug-related conditions. Furthermore, it is more difficult to diagnose PD at this early stage since its clinical signs may be mild and unnoticed (5,6). Therefore, *in vivo* markers of dopaminergic degeneration are essential for early diagnosis and disease progression monitoring. A radioactive tracer, 6-^{18}F-fluoro-L-dopa (^{18}F-FDOPA), has been extensively used in positron emission tomography (PET) brain image studies to assess the presynaptic nigrostriatal dopaminergic function. The uptake of ^{18}F-FDOPA PET demonstrates the activity of the dopa-decarboxylase enzyme in the striatal nerve terminals of dopamine neurons and is correlated with the dopamine storage capacity (7,8,9).

A nuclear medicine physician interprets the ^{18}F-FDOPA PET imaging based on the visualization of the relative radioactivity distribution in the striatum. A decreased ^{18}F-FDOPA uptake in the striatum contralateral to the side of the main or first motor symptoms (due to crossing of the pyramidal pathway) has been reported in early PD patients (10,11,12,13,14,15). The depletion is more severe in the putamen than in the caudate nucleus. The most prominent depletion is in the dorsal parts of the putamen because of the topographic organization of the nigrostriatal projection (4,11,16). Most previous studies differentiate PD from non-PD based on the qualitative assessment or semi-quantitative analysis, such as the standardized uptake value or reference tissue-uptake ratio as an imaging biomarker. However, these studies have not identified any sensitive parameters derived from kinetic modeling in the striatal subregion. The quantitative analysis of biokinetic data in ^{18}F-FDOPA PET brain imaging may provide additional clinical usefulness to the routine qualitative assessment, especially when the qualitative analysis could not differentiate PD from non-PD conditions.

There are several pharmacokinetic (PK) approaches in PET imaging techniques, of which compartmental modeling has been used to simulate the physiologically significant parameters. In compartmental models, the organ of interest is composed of many interacting subsystems (compartments) with a set of transfer rate constants describing the exchanges of mass or material between the compartments (17,18,19,20,21,22). Wahl and Nahmias (22) published a simplified two-tissue compartment, three-rate constant ^{18}F-FDOPA kinetic model by eliminating the fourth transfer rate constant and the number of compartments. The significant difference between normal subjects and PD patients was found in the dopa-decarboxylase rate constant (k_3). However, only two patients were investigated, and the stages of the PD were not clearly defined.

This study aimed to investigate the transfer rate constants of ^{18}F-FDOPA in the brain PET images of patients with early-stage PD, based on the compartmental modeling of Wahl and Nahmias, and to identify optimal quantitative parameters that could differentiate between normal and pathological FDOPA metabolism. Furthermore, we aimed

to re-evaluate if a two-tissue compartment, three-rate constant PK model could adequately describe the FDOPA kinetics and its metabolite in the striatal, caudate, and putamen of patients with early PD.

Materials and Methods

Patients and ^{18}F-FDOPA Image Acquisition

This study was approved by the Institutional Review Board (IRB) of the Faculty of Medicine, Chulalongkorn University (IRB no. 361/61). In consultation with the IRB, the use of already collected and anonymized imaging data for this study was deemed exempt from formal informed consent. Retrospective data were collected from five patients who underwent an ^{18}F-FDOPA PET brain scan at the Division of Nuclear Medicine, King Chulalongkorn Memorial Hospital (KCMH). All patients were diagnosed with stage II PD according to the Hoehn and Yahr (HY) staging (23) and the UK PD Society Brain Bank Clinical Diagnosis Criteria (24). Patients' demographic and clinical data are shown in Table 1. All patients fasted for 4-6 h before the FDOPA injection. Patients who had drug-induced parkinsonian syndrome or vascular causes of parkinsonian syndrome were excluded from this study. All patients were treated with levodopa in combination with FDOPA decarboxylase inhibitor (carbidopa). The patient preparation protocol for the ^{18}F-FDOPA PET neurological imaging at the KCMH was followed the joint practice guideline developed collaboratively by the European Association of Nuclear Medicine (EANM) and the Society of Nuclear Medicine and Molecular Imaging (SNMMI) (25,26). The protocol required that carbidopa and other anti-parkinsonian drugs must be discontinued 2 days before the examination to ensure that there is no interpretation bias because of the carbidopa effect from the FDOPA accumulation in the striatal region. A nuclear medicine physician interpreted the PET images. Typical early PD was identified when the visual assessment revealed a relatively unilateral decrease in ^{18}F-FDOPA uptake in the dorsal part of the putamen.

Three-dimensional list-mode brain PET data were acquired for 90 min using the Siemens Biograph 16 HI-REZ PET/CT system (CTI/Siemens Medical Solutions, Knoxville, TN, USA) immediately after patients were intravenously injected with 306-379 MBq ^{18}F-FDOPA. A series of PET images were reconstructed using an ordered subset expectation maximization algorithm with four iterations and 14 subsets, matrix size of 168x168, and voxel size of 4.0627x4.0627x3 mm^3 to obtain a 90-min dynamic image with the framing scheme of 18x5 min frames. Decay, attenuation, model-based scatter corrections, and 5-mm Gaussian filter of convolution kernel were applied for all PET image reconstruction.

Striatal Segmentation using the Statistical Parametric Mapping (SPM)

To achieve the consistency of region of interest (ROI) contouring in the striatum, caudate, and putamen, all subsequent image manipulations and data analyses were performed using the SPM software. Before the contouring process, Digital Imaging and Communications in Medicine image files were converted into an interfile format using the MRICRON software to create SPM-compatible images. The images were then imported into the SPM software version 12 (27), which was operated on the MATLAB software version R2018a (Mathworks, Natick, MA, USA). The images were reoriented as close as possible to the magnetic resonance (MR) reference images by adjusting the individual movement parameters (pitch, roll, and yaw), and the crosshair origin (0, 0, 0) was checked to be closed to the anterior commissure.

The series of reoriented images were coregistered and stereotactically normalized with the International Consortium for Brain Mapping (ICBM) using 16 iterations of nonlinear warping, a frequency cut-off at 25, and 8-mm full-width at half maximum Gaussian filter as a smoothing filter. The initial image parameters were 168x168x109, which resulted in a 16-bit final image format with a size of 181x217x181 and a voxel size of 1x1x1 mm^3. The normalized images were then segmented automatically

Table 1. The patient' demographic and clinical data

Patient	Age (years)	Weight (kg)	Sex	Administered activity (MBq)	Severity (HY scale)	Lower uptake striatum (side)[a]	Affected side	Initial symptom
1F	75	80	Female	358	II	Left	Right	Tremor
2F	64	57	Female	306	II	Left	Right	Tremor
3F	62	54	Female	323	II	Left	Right	Rigidity/tremor
4M	44	76	Male	379	II	Left	Right	Tremor
5F	71	50	Female	349	II	Left	Right	Bradykinesia/rigidity

[a]Lower uptake level of ^{18}F-FDOPA, HY: Hoehn and Yahr, ^{18}F-FDOPA: ^{18}F-fluoro-L-dopa

into the striatum, caudate, and putamen by making a binary mask image from the Automated Anatomical Labeling-VOIs atlas, which was derived from the Montreal Neurological Institute (MNI) T1-MR imaging (MRI) data set. The image segmentation was performed in each single frame of the patient data set. A PET template of the ICBM used in the coregistration and stereotactical normalization was derived from the perfusion ^{15}O-labeled water. The overall orientation was matched with MNI space templates, and a nuclear medicine physician visually validated the delineation results in these striatal subregions to confirm that the segmentation utilizing the SPM was performed appropriately. The overall process of the semi-automated segmentation in the striatum, caudate, and putamen using SPM is illustrated in Figure 1.

Determination of the Scaling Factor for Activity Concentration

Changes in pixel values during the SPM processing may occur on the original and normalized images after applying the coregistration and normalization. The scaling factor was determined to correct the changes. A whole-brain image histogram was computed at each time point using the ImageJ program. The histogram provided the mean and count values, which referred to the activity concentration (Bq/mL) and the total number of voxels, respectively. The whole-image activity (Bq) in each time frame was determined by multiplying these values and the voxel volume (0.0248 and 0.001 mL in the original and normalized images, respectively). The whole-brain image activity from the original images was then divided by the respective normalized images to determine the mean value from all time frames, and the mean scaling factors were computed.

To determine the radioactivity in the striatum, caudate, and putamen, the rectangular ROIs were manually drawn over these three regions on each side to compute the histogram in each time frame as illustrated in Figure 2. The whole-region activity (Bq) was calculated by multiplying the activity concentration with the total voxel number, voxel volume (0.001 mL), and mean scaling factor. The whole-region activity (Bq) in every time frame of the striatum,

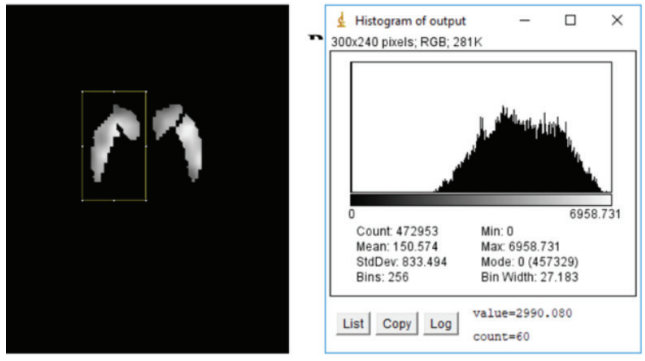

Figure 2. (Left) region of interest over right side of the striatum, and (right) the histogram output

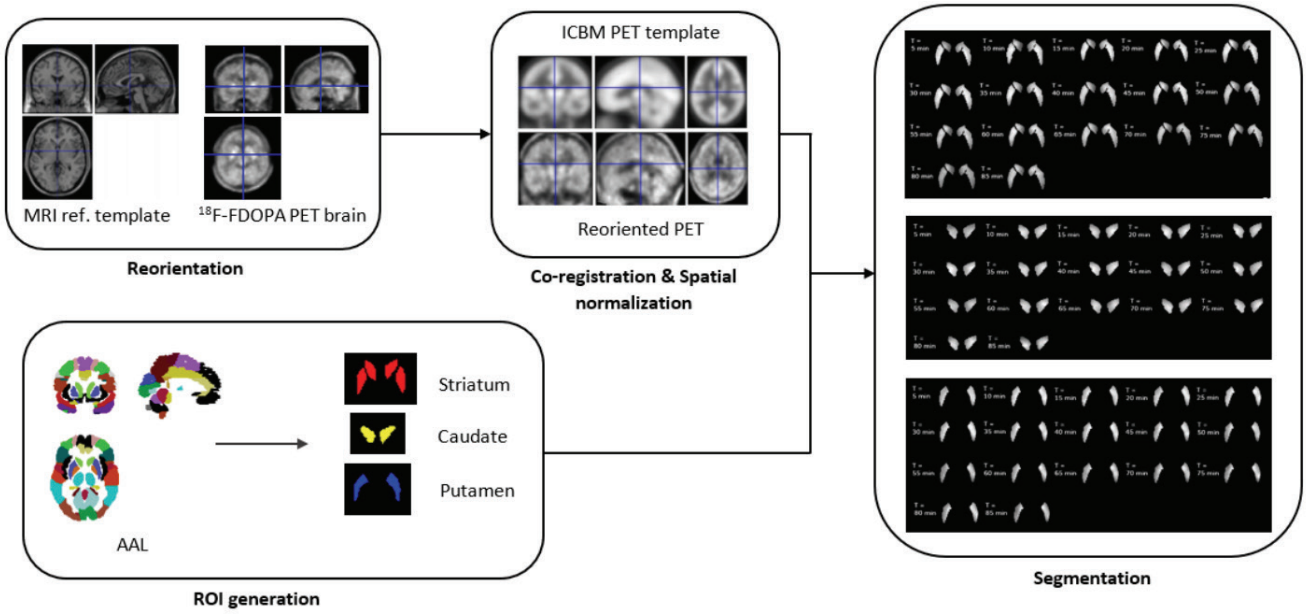

Figure 1. Schematic flowchart showing the semi-automated segmentation in the striatum, caudate, and putamen regions using the statistical parametric mapping (SPM)

MRI: Magnetic resonance imaging, ^{18}F-FDOPA: ^{18}F-fluoro-L-dopa, PET: Positron emission tomography, ICBM: International Consortium for Brain Mapping

caudate, and putamen was obtained from each side. The results of the ipsilateral versus contralateral to the predominant motor symptoms were calculated separately. The analysis between the PD and control was performed within the same patient. The contralateral side that had lower uptake was identified as the PD, and the ipsilateral side (normal uptake) as the control.

^{18}F-FDOPA Compartmental Model for PD Patients

A two-tissue compartment, three-rate constant model was chosen for a PK ^{18}F-FDOPA model in this study. The percentage of the injected radioactivity was calculated every 5 min after injection in each region. Data were imported into the SAAM II compartmental modeling software (The Epsilon Group, Charlottesville, VA, USA) (28). The FDOPA PK compartmental model was created and followed the Wahl and Nahmias'(22) model as shown in Figure 3. The model was fitted to the PD patient data. The model fitting was initially performed using the rate constants reported by Wahl and Nahmias (22). Then, the SAAM II software computationally created a system of ordinary differential equations, according to the specified compartmental model structure, and simulated the solutions based on the provided parameters and model inputs. The image-based input function to the model (bolus injection into the blood) for the compartment analysis in this study can be defined as follows:

$$\text{Input function} = ((q_3+q_4)*BVF*(a*q_1+(1-a)*q_2))*\exp(-\log(2)*t/110), \quad (1)$$

where q_i is the ^{18}F-FDOPA activity in the i^{th} compartment; q_1, q_2, q_3, and q_4 are the ^{18}F-FDOPA activities that internally solved differential equations by SAAM II in plasma, erythrocytes, FDOPA brain tissue, and its metabolite compartments, respectively. BVF refers to an estimate of blood volume fraction in the brain tissue, and *a* is the coefficient value assumed to be 0.6; t is the ^{18}F physical half-life of 109.7 min. The general assumption in SAAM II was that the flux of material between compartments depended only on the amount of material presented in the starting compartment (29). This corresponded to the assumption of first-order kinetics. The transfer rate constants of FDOPA exchanging between the compartments, which were created internally and solved by SAAM II, were described by the following set of differential equations:

$$\frac{dC_{Tissue}(t)}{d(t)} = K_1C_{plasma}(t)-k_2C_{Tissue}(t)-k_3C_{Tissue}(t), \quad (2)$$

$$\frac{dC_{FDA}(t)}{d(t)} = k_3C_{Tissue}(t), \quad (3)$$

where C_{Tissue} and C_{FDA} represent radioactivity concentrations of the tissue FDOPA and 6-[^{18}F] fluorodopamine (FDA) and its metabolites compartment, respectively. K_1 and k_2 are the forward and reverse transport rate constants of plasma FDOPA across the blood–brain barrier to the tissue FDOPA compartment, whereas k_3 represents the FDOPA decarboxylation rate constant from the tissue FDOPA compartment to the combined compartment of FDA and its metabolites. The SAAM II then generated a time-integrated activity curve of the model and fitted it to the patient data based upon a nonlinear least square regression algorithm. The transfer rate constants (K_1, k_2, and k_3) in each patient were determined accordingly.

To assess the performance of model fitting, the Akaike information criterion (AIC) and the Bayes information criterion (BIC) were used to assess which of the rate constants would best fit the patient's data. The AIC is a technique based on in-sample fit to estimate the likelihood of a model to predict the values. The BIC is another criterion for model selection that measures the trade-off between the model fit and complexity of the model. Lower AIC and BIC values indicated a better fit. The AIC and BIC values can be determined using equations as follows (30,31):

$$AIC = 2k-2(\ln)(L), \quad (4)$$

$$BIC = k(\ln)(N)-2(\ln)(L), \quad (5)$$

where L is the value of the likelihood, N is the number of recorded measurements, and k is the number of estimated parameters. As a result, the parameter with minimum AIC and BIC values was chosen as the best fitting model among several competing models.

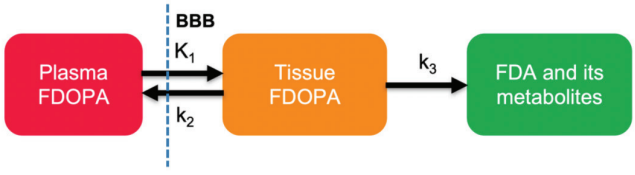

Figure 3. Two-tissue-compartment and three-rate constant for describing the FDOPA kinetics in early PD patients following Wahl and Nahmias (22)

FDOPA: Fluoro-L-dopa, PD: Parkinson's disease, FDA: Fluorodopamine

Statistical Analysis

The transfer rate constants (K_1, k_2, and k_3) in each region were determined. The comparisons between the ipsilateral and contralateral sides of the striatum, caudate, and putamen were performed using a non-parametric statistic, the Wilcoxon signed-rank test. Data analysis was performed using the Statistical Package for Social Sciences program version 23 (IBM Corp, Armonk, NY, USA). The differences

between groups were considered significant when p values were less than 0.05.

Results

Figure 4 depicts the mean time-activity curves after the ^{18}F-FDOPA injection obtained from both the ipsilateral and contralateral sides of the striatum (Figure 4A), caudate (Figure 4B), and putamen (Figure 4C). The activity uptake in each region was expressed as a percentage of the injected radioactivity and represented by a range (mean ± standard deviation) as follows: (a) The striatum 0.0225%-0.0453% (0.0323±0.0091) and 0.0263%-0.0457% (0.0353±0.0086) for the contralateral and ipsilateral sides, respectively, (b) the caudate 0.0112-0.0204% (0.0155±0.0038) and 0.0118%-0.0191% (0.0154±0.0034), and (c) the putamen 0.0113%-0.0249% (0.0169±0.0054) and 0.0139%-0.0273% (0.0199±0.0054). The highest average percentage of injected activity was at 15 min after injection in every region.

According to the PK model fitting, the measured FDOPA curves fitted well to a two-tissue compartment, three-rate constant model (mean AIC of -5.72 and BIC of -5.62). The time-activity curves of both sides initially increased after the injection, reached the maximum uptake activity at 15 min after injection, and then decreased slightly thereafter. The activity uptakes on the contralateral side of the striatum and putamen were significantly lower than the ipsilateral side. However, the caudate time-activity curves were nearly superimposed on each other (Figure 4).

The details of the transfer rate constants on the contralateral and ipsilateral sides are presented in Table 2. Figures 5A and 5B depict the box plot of the transfer rate constants for both sides of the striatum and putamen. There were statistically significant differences in K_1 and k_3 between the contralateral and ipsilateral sides of the striatum and putamen ($p<0.05$). However, there were no significant differences in the k values between both sides of the caudate region (not shown).

Figure 6 illustrates the ^{18}F-FDOPA PET transaxial images from a patient suspected of idiopathic parkinsonism with right-hand resting tremor (patient no: 1). Based on visual interpretation, there was a subtle change of relatively mild decreased ^{18}F-FDOPA uptake at the dorsal part of the left putamen and symmetrical uptakes at the bilateral caudate nuclei. After quantitative analysis using the PK model was applied for further confirmation, the K_1 (0.0109 vs. 0.0124) and k_3 (0.0098 vs. 0.0146) of the contralateral putamen were significantly lower than that of the ipsilateral side. This quantitative analysis provided the results that supported the visual assessment.

Discussion

This study investigated the transfer rate constants of ^{18}F-FDOPA in the PET brain images of five early PD patients. The PK model in this study was a two-compartmental, three-transfer rate constants model, which was based on compartmental modeling in accordance with Wahl and Nahmias (22). The results demonstrated the differences between the contralateral and ipsilateral sides of the striatum, including the caudate and putamen, which was in agreement with Wahl and Nahmias (22). The mean transfer rate constants K_1 and k_3 on the contralateral (PD) striatum and putamen were significantly lower than those on the ipsilateral (normal) side ($p<0.05$). In addition, the difference was more pronounced in the putamen. In contrast, no significant differences were found in the caudate. These findings agreed with the results of previous PD imaging studies, which suggested that the dopamine

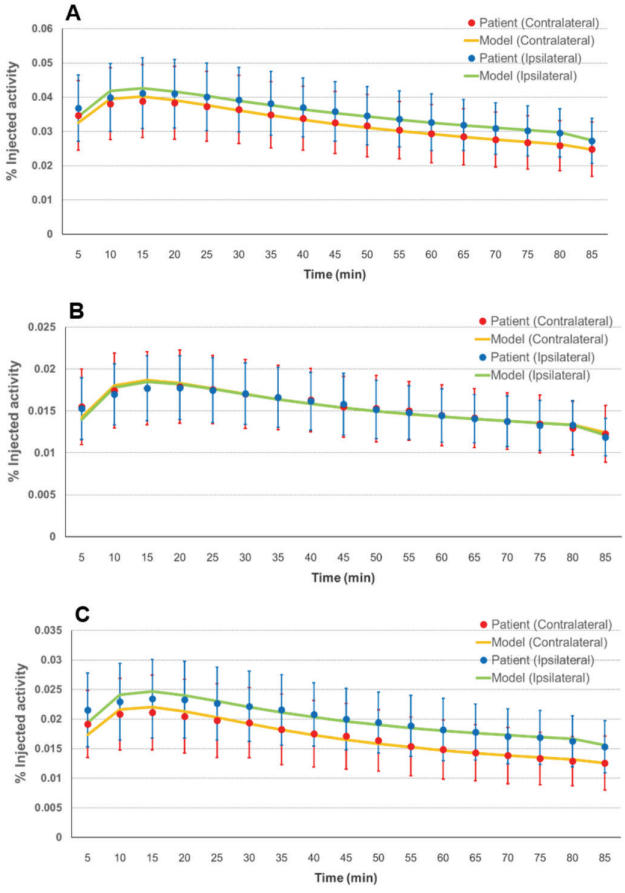

Figure 4. Mean (± 1 SD) time-activity curves in the (A) striatum, (B) caudate, and (C) putamen. Blue and red round markers represent patient's data obtained from the contralateral and ipsilateral side, respectively. Green and yellow lines represent the model fitted from the contralateral and ipsilateral side, respectively

SD: Standard deviation

depletion began in the dorsal parts of the putamen and proceeded to the caudate nucleus and other parts of the dopaminergic system during disease progression (4,11,16). The decreased ^{18}F-FDOPA uptake in this work was more significant in the contralateral striatum, which was in accordance with an observation that the motor symptoms were more severe on the contralateral side to the striatum that had decreased dopaminergic activity (3). However, our results may only represent patients with stage two of PD who had right-side predominant symptoms (Table 1) or loss of activity uptake in the left striatum.

Table 3 illustrates the transfer rate constants of this work compared with previous reports by Huang et al. (21) and Wahl and Nahmias (22). Wahl and Nahmias (22) found a significant difference in the dopa-decarboxylase rate constant between normal subjects and PD patients, although only two PD patients were investigated. The FDOPA transfer rate constants for K_1 and k_2 of the ipsilateral (normal) side in our study were approximately two-fold lower than those of Wahl and Nahmias' study but were comparable with Huang's study. The patient characteristics could be the cause of the differences in these transfer rate constants. The k_3 of the contralateral (PD) striatum in our study was 2.6-fold higher than in Wahl and Nahmias' study. This might be explained by the difference in the severity of PD between the studies. This study was conducted in early PD patients with distinct inclusion criteria following an HY score limited to 2. Therefore, the loss of dopaminergic neurons in our patients may be less than the patients in the Wahl and Nahmias' study. Although the clinical rating scale of the patients had not been described in the Wahl and Nahmias' study, their results implicitly indicated that the patients might suffer from late stages of PD (HY stage 3 or 4).

The finding in this work indicated that in addition to k_3, K_1 was likely to be another sensitive parameter to differentiate PD and normal patients. The difference in the results compared with previous studies was possibly

Table 2. The estimated FDOPA model parameters in the contralateral and ipsilateral sides

	Contralateral side (PD)			Ipsilateral side (normal)		
	K_1 (mL/min/g)	k_2 (/min)	k_3 (/min)	K_1 (mL/min/g)	k_2 (/min)	k_3 (/min)
Striatum						
Patient 1	0.0221	0.0155	0.0064	0.0242	0.0159	0.0111
Patient 2	0.0254	0.0203	0.0165	0.0268	0.0125	0.0210
Patient 3	0.0357	0.0163	0.0079	0.0363	0.0168	0.0088
Patient 4	0.0170	0.0287	0.0105	0.0192	0.0283	0.0159
Patient 5	0.0154	0.0171	0.0146	0.0160	0.0154	0.0195
Mean (SD)	0.0231 (0.0081)	0.0196 (0.0054)	0.0112 (0.0043)	0.0245 (0.0078)	0.0178 (0.0061)	0.0152 (0.0053)
Caudate						
Patient 1	0.0095	0.0214	0.0129	0.0096	0.0228	0.0163
Patient 2	0.0104	0.0258	0.0315	0.0109	0.0251	0.0352
Patient 3	0.0137	0.0317	0.0246	0.0113	0.0201	0.0121
Patient 4	0.0071	0.0265	0.0144	0.0077	0.0264	0.0171
Patient 5	0.0061	0.0130	0.0183	0.0061	0.0193	0.0270
Mean (SD)	0.0094 (0.0030)	0.0237 (0.0070)	0.0203 (0.0077)	0.0091 (0.0022)	0.0228 (0.0031)	0.0215 (0.0094)
Putamen						
Patient 1	0.0109	0.0209	0.0098	0.0124	0.0211	0.0146
Patient 2	0.0128	0.0301	0.0148	0.0136	0.0203	0.0208
Patient 3	0.0173	0.0214	0.0081	0.0202	0.0286	0.0161
Patient 4	0.0087	0.0344	0.0094	0.0102	0.0366	0.0174
Patient 5	0.0084	0.0272	0.0142	0.0090	0.0204	0.0191
Mean (SD)	0.0116 (0.0037)	0.0268 (0.0057)	0.0113 (0.0030)	0.0131 (0.0044)	0.0254 (0.0072)	0.0176 (0.0025)

FDOPA: Fluoro-L-dopa, SD: Standard deviation, PD: Parkinson's disease

because of the data collection method. The simulation of the PK model fitted to the patient's data in this work was an image-based analysis acquired from radioactivity uptake in the striatal region, whereas previous reports collected the data based on a combination of arterialized venous blood sampling and image analysis. Although the biochemical assay method may be preferable, the image-based analysis could be better and more convenient in ^{18}F-FDOPA PET quantification. It is less invasive, has reduced occupational dose and complexity, and can provide retrospective data. It was noticeable that PD patients had stopped taking the FDOPA decarboxylase inhibitor 2 days before the imaging examination. The elimination half-life of carbidopa in plasma is approximately 107 min. Two days of drug discontinuation should be long enough to ensure that there was no visual interpretation bias due to the carbidopa effect on the physiological uptake in the striatum.

This study did not include healthy volunteers as the control group. The striatum contralateral side to the main symptoms that had a lower ^{18}F-FDOPA uptake was considered to be PD and the other side of the same patient

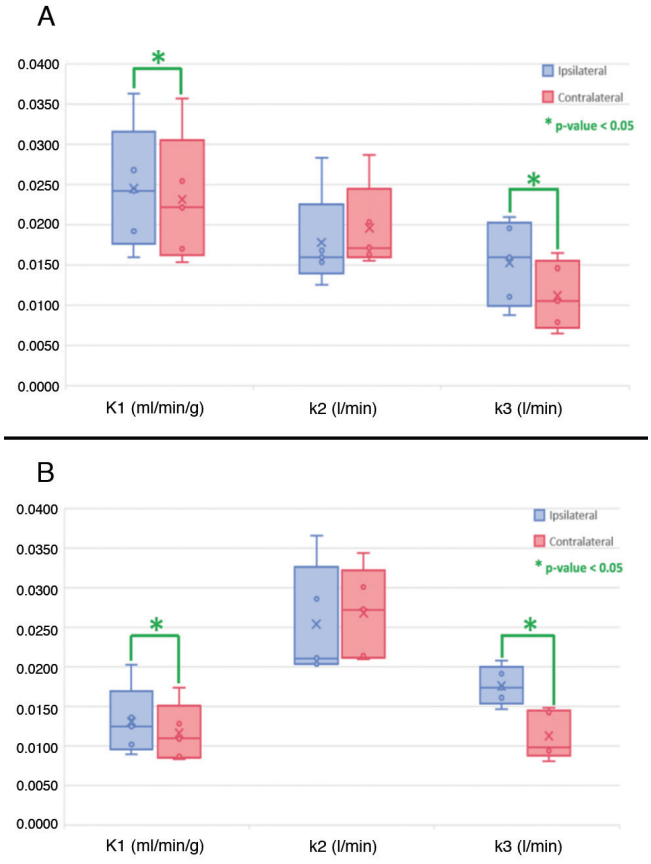

Figure 5. Box plots of the transfer rate constants in the contralateral (red) and ipsilateral (blue). (A) striatum and (B) putamen

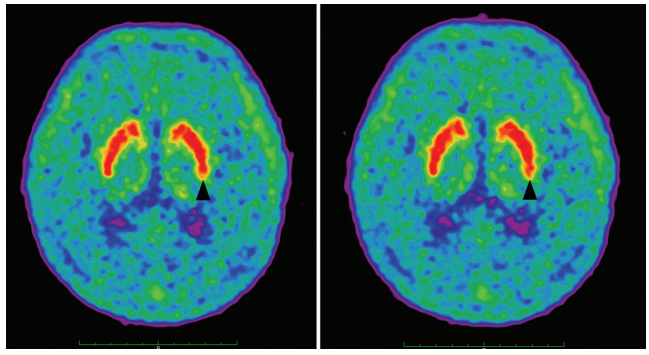

Figure 6. Example of static ^{18}F-FDOPA PET images in a case of the early PD with HY rate stage II. The arrows indicate the relatively mild decreased FDOPA uptake demonstrated by the red light shading at the dorsal part of left posterior putamen

^{18}F-FDOPA: ^{18}F-fluoro-L-dopa, PET: Positron emission tomography, PD: Parkinson's disease, HY: Hoehn and Yahr

Table 3. Comparison of transfer rate constants between earlier reports and this study			
Study	Huang et al. (21)	Wahl and Nahmias (22)	This study
Overall demographic			
Subjects	Normal: 10	Normal: 4, PD: 2	PD: 5
HY stage	N/A	Late	Early
Average (SD) transfer rate constants in the ipsilateral striatum (normal)			
K_1 (mL/min/g)	0.0283 (0.0051)	0.0403 (0.0177)	0.0245 (0.0078)
k_2 (/min)	0.0228 (0.0048)	0.0342 (0.0185)	0.0178 (0.0061)
k_3 (/min)	0.0124 (0.0041)	0.0124 (0.0058)	0.0152 (0.0053)
Average (SD) transfer rate constants in the contralateral striatum (PD)			
K_1 (mL/min/g)	N/A	0.0494 (0.0072)	0.0231 (0.0081)
k_2 (/min)		0.0281 (0.0072)	0.0196 (0.0054)
k_3 (/min)		0.0043 (0.0010)	0.0112 (0.0043)
HY: Hoehn and Yahr, PD: Parkinson's disease, SD: Standard deviation, N/A: Not applicable			

was non-PD. We elaborately recruited the typical type of early PD patients following the inclusion and exclusion criteria suggested by nuclear medicine experts and the joint EANM/SNMMI procedure guidelines (25). All patients were followed up and clinically diagnosed with early PD. Hence, the uniform uptake of FDOPA at the caudate and putamen on the ipsilateral side was assumed as a normal reference in the same patient. The comparison within the same patient would possibly eliminate the variables from cross-patient studies. However, the sensitivity of this asymmetry method depended on the degree of difference between each side. Moreover, the cases with symmetric involvement would be missed even if the abnormality is substantial. Further study on biokinetic data comparing healthy subjects or patients with non-neurodegenerative parkinsonism is required to confirm the results of this work.

The striatal delineation approach using SPM in this study was also performed to improve the reproducibility of striatal subregion segmentation. In the process of reorienting images, the patient's own MRI should be used to roughly align structural images with standard space for coregistration before automated subcortical structures segmentation using SPM. However, some patients in this study did not have their own MRI brain scans. To address this drawback, we used the standard MRI provided by the SPM to reorient the PET images before tissue class segmentation. Although this approach might not be perfect, the uncertainty was acceptable for keeping the consistency in the reorienting process. This approach provided the segmented subregions in every patient with the same volume (Figure 1) and might not yield a perfect coregistration and segmentation accordingly.

Study Limitations

This limitation may lead to variations in the ^{18}F-FDOPA quantification in brain tissues for generating the time-activity curve to simulate the kinetic model.

Conclusion

The two-tissue compartmental model with three-transfer rate constants was able to describe ^{18}F-FDOPA kinetics in the striatum, caudate, and putamen, which was consistent with earlier studies. The K_1 and k_3 transfer rate constants of ^{18}F-FDOPA in the striatum and putamen on the contralateral side to the patient's symptom were significantly lower than the control. The K_1 and k_3 could be potential indicators for quantitative detection to improve early PD diagnosis. These findings provided more insight of the FDOPA PKs for PD patients and could be useful in clinical practice.

Acknowledgements

The authors would like to thank Mr. Natakorn Siritranont for his help on imaging data collection. The authors would also like to thank the nuclear medicine technologists, medical physicists, and nuclear medicine physicians at the Division of Nuclear Medicine, KCMH, and Chulalongkorn University for their kind support in this study. We deeply thank Associate Professor Dr. Shuichi Shiratori for his valuable advice in the FDOPA mechanism. We also thank Professor Dr. Roongroj Bhidayasiri from Chulalongkorn Center of Excellence for PD and Related Disorders for the valuable PD patient information. This work was funded by Chulalongkorn University, government budget (GB-A_61_006_30_02), and the Thailand Research Fund (MRG6180141). Miss Wirunpatch Buratachwatanasiri was supported by a Graduate School Scholarship, the Faculty of Medicine, Chulalongkorn University, Thailand.

Ethics

Ethics Committee Approval: This study was approved by the Institutional Review Board (IRB) of the Faculty of Medicine, Chulalongkorn University (IRB no. 361/61).

Informed Consent: The use of already collected, anonymized, imaging data for the purposes of this study was deemed exempt from the formal informed consent by the IRB of our institution.

Peer-review: Externally and internally peer-reviewed.

Authorship Contributions

Concept: K.K., W.B., M.C., Design: K.K., W.B., Data Collection or Processing: W.B., Y.R., J.O., Analysis or Interpretation: W.B., K.K., M.C., Y.C., Literature Search: K.K., W.B., Writing: K.K., W.B.

Conflict of Interest: No conflict of interest was declared by the authors.

Financial Disclosure: This work was funded by the government budget (GB-A_61_006_30_02) Chulalongkorn University, and the Thailand Research Fund (MRG6180141).

References

1. DeMaagd G, Philip A. Parkinson's Disease and Its Management: Part 1: Disease Entity, Risk Factors, Pathophysiology, Clinical Presentation, and Diagnosis. P T 2015;40:504-532.
2. Antić S, Lisak M, Trkanjec Z, Demarin V. Parkinsonova bolest. Acta Clin Croat 2009;48:377-380.
3. Lang AE, Lozano AM. Parkinson's disease. New England Journal of Medicine. 1998;339:1130-1143.
4. Brooks DJ. Neuroimaging in Parkinson's disease. NeuroRx 2004;1:243-254.

5. Sawle GV. The detection of preclinical Parkinson's disease: What is the role of positron emission tomography? Movement disorders: official journal of the Movement Disorder Society 1993;8:271-277.
6. Hughes AJ, Daniel SE, Kilford L, Lees AJ. Accuracy of clinical diagnosis of idiopathic Parkinson's disease: a clinico-pathological study of 100 cases. J Neurol Neurosurg Psychiatry 1992;55:181-184.
7. Kumakura Y, Gjedde A, Danielsen EH, Christensen S, Cumming P. Dopamine storage capacity in caudate and putamen of patients with early Parkinson's disease: correlation with asymmetry of motor symptoms. J Cereb Blood Flow Metab 2006;26:358-370.
8. Leung K. L-3, 4-Dihydroxy-6-[18F] fluorophenylalanine. In: Molecular Imaging and Contrast Agent Database (MICAD)[Internet]. National Center for Biotechnology Information (US); 2011.
9. Nanni C, Fanti S, Rubello D. 18F-DOPA PET and PET/CT. J Nucl Med 2007;48:1577-1579.
10. Kish SJ, Shannak K, Hornykiewicz O. Uneven pattern of dopamine loss in the striatum of patients with idiopathic Parkinson's disease. Pathophysiologic and clinical implications. N Engl J Med 1988;318:876-880.
11. Brück A, Aalto S, Nurmi E, Vahlberg T, Bergman J, Rinne JO. Striatal subregional 6-[18F] fluoro-L-dopa uptake in early Parkinson's disease: a two-year follow-up study. Mov Disord 2006;21:958-963.
12. Lotankar S, Prabhavalkar KS, Bhatt LK. Biomarkers for Parkinson's Disease: Recent Advancement. Neurosci Bull 2017;33:585-597.
13. Sung YH, Lee J, Nam Y, Shin HG, Noh Y, Shin DH, Kim EY. Differential involvement of nigral subregions in idiopathic parkinson's disease. Hum Brain Mapp 2018;39:542-553.
14. Morrish PK, Sawle GV, Brooks DJ. Clinical and [18F] dopa PET findings in early Parkinson's disease. J Neurol Neurosurg Psychiatry 1995;59:597-600.
15. Yagi S, Yoshikawa E, Futatsubashi M, Yokokura M, Yoshihara Y, Torizuka T, Ouchi Y. Progression from unilateral to bilateral parkinsonism in early Parkinson disease: implication of mesocortical dopamine dysfunction by PET. J Nucl Med 2010;51:1250-1257.
16. Chang IC, Lue KH, Hsieh HJ, Liu SH, Kao CH. Automated striatal uptake analysis of ^{18}F-FDOPA PET images applied to Parkinson's disease patients. Ann Nucl Med 2011;25:796-803.
17. Morris ED, Endres CJ, Schmidt KC, Christian BT, Muzic RF, Fisher RE. Kinetic modeling in positron emission tomography. Emission Tomography: The Fundamentals of PET and SPECT Academic, San Diego. 2004.
18. Nelissen N, Warwick J, Dupont P. Kinetic modelling in human brain imaging. Positron Emission Tomography. Current Clinical and Research Aspects 2012:978-953.
19. Seo Y, Teo BK, Hadi M, Schreck C, Bacharach SL, Hasegawa BH. Quantitative accuracy of PET/CT for image-based kinetic analysis. Med Phys 2008;35:3086-3089.
20. Watabe H, Ikoma Y, Kimura Y, Naganawa M, Shidahara M. PET kinetic analysis—compartmental model. Ann Nucl Med 2006;20:583-588.
21. Huang SC, Yu DC, Barrio JR, Grafton S, Melega WP, Hoffman JM, Satyamurthy N, Mazziotta JC, Phelps ME. Kinetics and modeling of L-6-[18F]fluoro-dopa in human positron emission tomographic studies. J Cereb Blood Flow Metab 1991;11:898-913.
22. Wahl L, Nahmias C. Modeling of fluorine-18-6-fluoro-L-Dopa in humans. J Nucl Med 1996;37:432-437.
23. Bhidayasiri R, Tarsy D. Parkinson's disease: hoehn and yahr scale. In: Movement Disorders: A Video Atlas. Springer; 2012:4-5.
24. Hughes A, Ben-Shlomo Y, Daniel S, Lees A. UK Parkinson's disease society brain bank clinical diagnostic criteria. J Neurol Neurosurg Psychiatr 1992;55:e4.
25. Darcourt J, Booij J, Tatsch K, Varrone A, Vander Borght T, Kapucu OL, Någren K, Nobili F, Walker Z, Van Laere K. EANM procedure guidelines for brain neurotransmission SPECT using (123)I-labelled dopamine transporter ligands, version 2. Eur J Nucl Med Mol Imaging 2010;37:443-450.
26. Morbelli S, Esposito G, Arbizu J, Barthel H, Boellaard R, Bohnen NI, Brooks DJ, Darcourt J, Dickson JC, Douglas D, Drzezga A, Dubroff J, Ekmekcioglu O, Garibotto V, Herscovitch P, Kuo P, Lammertsma A, Pappata S, Peñuelas I, Seibyl J, Semah F, Tossici-Bolt L, Van de Giessen E, Van Laere K, Varrone A, Wanner M, Zubal G, Law I. EANM practice guideline/SNMMI procedure standard for dopaminergic imaging in Parkinsonian syndromes 1.0. Eur J Nucl Med Mol Imaging 2020;47:1885-1912.
27. Ashburner J, Barnes G, Chen CC, Daunizeau J, Flandin G, Friston K, Jafarian A, Kiebel S, Kilner J, Litvak V, Moran R, Penny W, Razi A, Stephan K, Tak S, Zeidman P, Gitelman D, Henson R, Hutton C, Glauche V, Mattout J, Phillips C. SPM12 manual. Wellcome Trust Centre for Neuroimaging, London, UK. 2014:2464.
28. Barrett PH, Bell BM, Cobelli C, Golde H, Schumitzky A, Vicini P, Foster DM. SAAM II: Simulation, Analysis, and Modeling Software for tracer and pharmacokinetic studies. Metabolism 1998;47:484-492.
29. Tavola F, Janzen T, Giussani A, Facchinetti D, Veronese I, Uusijärvi-Lizana H, Mattsson S, Hoeschen C, Cantone MC. Nonlinear compartmental model of 18F-choline. Nucl Med Biol 2012;39:261-268.
30. Bozdogan H. Model selection and Akaike's information criterion (AIC): The general theory and its analytical extensions. Psychometrika 1987;52:345-370.
31. Schwarz G. Estimating the dimension of a model. The Annals of Statistics 1978;6:461-464.